Geoderma 356 (2019) 113925

Contents lists available at ScienceDirect

Geoderma

journal homepage: www.elsevier.com/locate/geoderma

# Evaluating sampling efforts of standard laboratory analysis and mid-infrared spectroscopy for cost effective digital soil mapping at field scale

S.S. Paul[a,*], N.C. Coops[b], M.S. Johnson[c], M. Krzic[a,d], S.M. Smukler[a]

[a] Soil Science Program, Faculty of Land and Food Systems, University of British Columbia, 2357 Main Mall, Vancouver, BC V6T 1Z4, Canada
[b] Department of Forest Resources Management, University of British Columbia, 2424 Main Mall, Vancouver, BC V6T 1Z4, Canada
[c] Institute for Resources, Environment and Sustainability, University of British Columbia, 2202 Main Mall, Vancouver, BC V6T 1Z4, Canada
[d] Department of Forest and Conservation Sciences, University of British Columbia, 2357 Main Mall, Vancouver, BC V6T 1Z4, Canada

ARTICLE INFO

Handling Editor: Alex McBratney

*Keywords:*
Standard laboratory analysis
High resolution environmental covariates
Conditioned Latin hypercube sampling
Kriging

ABSTRACT

The performance of digital soil mapping (DSM) model is highly reliant on the intensity and spatial distribution of the input soil data points. Increasing the number of soil data points (i.e. samples) improves the accuracy of the prediction, but it also raises the sampling effort, including the time, money and labor required for field and laboratory analysis. Thus, optimizing the production of DSMs requires maximizing accuracy while minimizing cost. In this study, we evaluated a range of strategies for DSM of a farm field using high spatial resolution ancillary environmental data (e.g. unmanned aerial vehicle-UAV imagery) and compared sampling efforts of soil data generated from standard laboratory analysis (SLA) and mid-infrared spectroscopy (MIRS) at equivalent costs. We produced DSMs of a number of soil properties including sand, silt, clay, pH, salinity, organic matter, and total nitrogen. We employed Conditioned Latin Hypercube Sampling (cLHS) to generate a range of sampling efforts from the full SLA ($n$ = 62) and MIRS ($n$ = 308) datasets and contrasted the DSM outcomes modeled using kriging with external drift (KED). We found that the DSM outputs were most effective, in terms of accuracy and cost, at 50–60% of the full sampling effort. Although MIRS predictions of soil properties introduced a sizable amount of error, DSMs produced using the MIRS dataset were more accurate as compared to the outcomes of SLA datasets at equivalent sampling efforts. The prediction accuracy for DSMs varied across the soil properties with $R^2$ ranging from 0.82 (for sand) to 0.45 (for total nitrogen) at the optimum sampling effort. The outcomes of the study highlight that spatially optimized sampling efforts and the use of the MIRS technique substantially improve the cost efficiency and accuracy of kriging-based DSM models for predicting a range of field scale soil properties.

## 1. Introduction

Digital soil mapping (DSM) is increasingly being used for managing and monitoring a wide range of soil-derived ecosystem services, including the provisioning of food, fiber and fuel, carbon sequestration and nutrient cycling. DSM combines information from sparsely populated point soil data with geospatial data, such as remotely sensed imagery, to provide continuous predictions of soil properties (Lagacherie, 2008; Li and Heap, 2011). DSM produces seamless spatial interpolation of point soil information at scales ranging from broad global maps to fine scale maps of individual farm fields (Grunwald et al., 2011; Malone et al., 2017). Detailed knowledge of soil properties at different scales can help land managers to make spatially explicit management decisions (Cruz-Cárdenas et al., 2014). Given that soil properties exhibit high spatial heterogeneity, mapping at finer spatial scales may be critical to meet specific farm management objectives, especially for precision agriculture (Malone et al., 2013; Suk Lee and Ehsani, 2015).

Fine scale DSM requires closely spaced point information (Hengl et al., 2004); however, there is no consensus regarding the sampling effort required for the optimum performance of the spatial prediction of soil properties (Brungard and Boettinger, 2010; Ließ, 2015). The number of samples, sample spacings, and the actual locations of the samples are all factors related to the sampling effort that influence the prediction process (Zhu and Lin, 2010). Enhancing the sampling effort by adding more samples will improve the accuracy of the predicted output, but this also increases time, cost and data processing required. Most sampling designs for DSM either aim to achieve a well-distributed spatial coverage of the area or to capture the spatial variations of the feature space (Minasny and McBratney, 2006). A number of studies on

* Corresponding author.
*E-mail address:* siddpaul@mail.ubc.ca (S.S. Paul).

https://doi.org/10.1016/j.geoderma.2019.113925
Received 5 April 2019; Received in revised form 12 August 2019; Accepted 22 August 2019

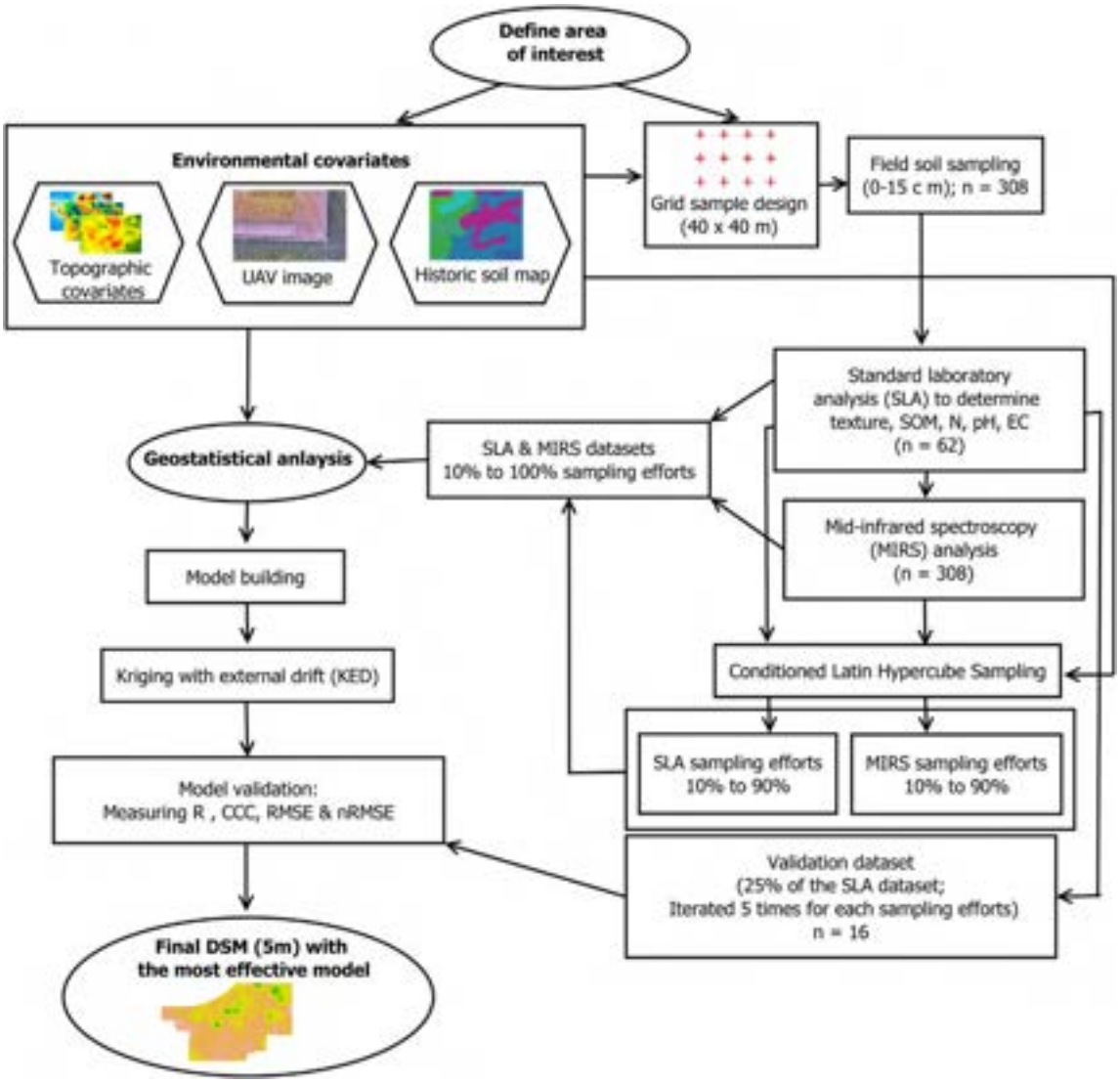


**Fig. 1.** Flowchart showing the methods utilized for producing digital soil maps (DSM) in this study. UAV refers to unmanned aerial vehicle; $R^2$, CCC, RMSE, and nRMSE refer to the coefficient of determination, Lin's concordance correlation coefficient, root mean square error, and normalized root-mean-square error respectively.

precision agriculture have explored this at the field scale and (Kerry et al., 2010) found that sampling interval of 100–120 m can provide adequate spatial coverage and precise soil management of a farm field. In order to achieve a well-distributed spatial coverage, the sampling effort may be increased but this does not necessarily result in accurate predictions. Alternatively, an optimum sampling effort may be obtained where the spatial variations of the study site can be effectively captured (Brungard and Boettinger, 2010). After reaching the optimum number of samples, increasing the number of samples will not improve the prediction capability of the model; rather, additional samples will result in diminishing returns in terms of improved accuracy of the model. Thus, a spatially optimized sampling effort will provide the most benefits in terms of both prediction accuracy and sampling investments.

The efficacy of the sampling design is likely dependant on the statistical model used for predicting the soil properties. Many studies have suggested that geospatial environmental variables are important for capturing spatial variations and improving the prediction accuracy of the models (Li et al., 2015). Kriging with external drift (KED) is one of the commonly used hybrid geostatistical models which assumes that the value at any given point is spatially dependent on the values of the neighboring points but the variation trend or drift is determined externally as a linear function of a group of ancillary environmental variables (Keskin and Grunwald, 2018; Wackernagel, 2003). KED, a straightforward approach where the trend and residuals are estimated as part of a single system, has been successfully used for a number of DSM studies where it obtained similar or better accuracies than simpler kriging models, like ordinary kriging (Li, 2010) or more complex and newer hybrid models, like regression kriging (Santra et al., 2017). Thus, KED can be used as an effective technique for predicting a suite of soil properties. The outcomes of KED prediction derived using various sampling designs can then be compared to identify the most effective sampling effort.

Standard laboratory analysis (SLA) of the soil samples can be a substantial portion of the overall DSM expense. Recent advances in soil analysis using mid-infrared spectroscopy (MIRS) have shown promise to reduce costs compared to SLA (Nocita et al., 2015). MIRS can produce fast and relatively inexpensive predictions of soil properties, that, although they are improving, are not as accurate as SLA as they are derived from SLA predictions (Viscarra Rossel et al., 2006). Larger sampling efforts, in general, better explain the spatial variability of the soil properties across a study site (Brus and Heuvelink, 2007). Thus, MIRS techniques, which allow the addition of more sample points for a

given budget, may make up for their reduced accuracy when producing predictive DSMs. Although MIRS techniques have recently been successfully used for landscape scale DSMs (Cobo et al., 2010; Vågen et al., 2016; Winowiecki et al., 2016), its performance in conjunction with field-scale DSM for a suite of soil properties is less clear. At the field scale, soil properties exhibit fine resolution spatial variations requiring a large set of soil data to produce accurate predictive maps. In precision agriculture, the use of visible- and near-infrared spectroscopy for on-the-go proximal soil sensing is widely used, however, use of MIRS is not common because of the high cost and lack of availability of portable MIRS instruments (Ge et al., 2011; Viscarra Rossel et al., 2006). Producing high resolution field scale DSM using laboratory based MIRS data could be an effective alternative to current proximal sensing approaches and/or demonstrate the utility of developing portable MIRS technology. However, there is a need to understand the trade-offs in accuracy and costs between using relatively more accurate, but more expensive SLA datasets and using comparatively less accurate, but less expensive MIRS datasets for DSM.

To address this research need, we conducted a study to produce digital maps of a suite of soil properties on a farm field in British Columbia at 5 m resolution using various approaches. The specific objectives of this study were to: (1) compare a range of equivalent sampling efforts (based on their cost for field work and lab analysis) of SLA and MIRS in terms of their relative accuracy for predicting a suite of soil properties, including sand, silt, clay, pH, salinity, soil organic matter (SOM), and total nitrogen (TN) and (2) assess the trade-offs between cost and accuracy to determine the most effective sampling effort for producing predictive maps of these soil properties.

## 2. Materials and methods

To develop DSMs of selected soil properties for a farm field in western Fraser Valley of British Columbia, we used a combination of methods (Fig. 1). We sampled soils using a grid design, then analyzed them using two different lab analysis approaches. We also applied multiple statistical and geostatistical tools to evaluate a range of sampling efforts (by pseudo-sampling from the full dataset) and the resulting DSM predictions for the soil properties.

### 2.1. Study site

The study site was a 54-hectare agricultural field near the City of Delta, British Columbia, Canada (49.08 N, 123.06 W), about 25 km south of the City of Vancouver (Fig. 2). The field had known salinity and drainage problems at the time of sampling and was used for organic vegetable production. The study site was located on Rego Gleysol and Orthic Humic Gleysol (Umbric Gleysol) formed predominantly from fluvial parent materials. The study site is in the Fraser River delta and close to the ocean with elevation ranges from 1.25 to 1.70 m above mean sea level. This area is characterized by a humid maritime climate with a mean annual temperature of 11.1 °C and a mean annual precipitation of 928 mm based on 30-year climate record (Environment Canada, 2019).

### 2.2. Soil sampling and analysis

After reviewing the existing soil map (Luttmerding, 1981) and conducting preliminary field observations, a 40 × 40 m grid was developed for soil sampling (Fig. 2). In 2015, a total of 308 points were sampled at the 0–15 cm depth across the field. All 308 sample locations were recorded with a GNSS Pro 6H Differential Global Positioning System (DGPS) (Trimble Inc., Sunnyvale, California, USA) with post-processing accuracy ranging from 10 to 50 cm. We derived a subsample set of the original 308 locations to use for SLA, and these were generally 120 m apart (compared to the original 40 × 40 m grid) but differed to a limited extent for some locations due to field edges. We included a few additional randomly selected grid locations for SLA analysis so that we achieve an equivalent cost for both SLA and MIRS. In total, 62 of the 308 original samples were retained for the SLA dataset.

All 308 samples were air dried and sieved to < 2 mm. The 62 SLA samples were sent to the Technical Service Laboratory of British Columbia Ministry of Environment for particle size analysis using the hydrometer method and for soil organic carbon (SOC) and TN using the combustion elemental analysis with a Vario EL Cube Elemental Analyzer (Elementar, Langenselbold, Germany). Separate aliquots of the subset of SLA samples was also analyzed at the University of British Columbia lab facility to measure pH in a 1:1 soil-water ratio, and electrical conductivity (EC) in a 1:2 soil-water ratio using an Oakton PC 700 pH/conductivity meter. The full 308 sample set was then analyzed with MIRS using a TENSOR 37 spectrometer (Bruker Instruments, Ettlingen, Germany). For MIRS analysis, the samples were prepared by oven drying at 105 °C before grinding with a ball-mill. We then analyzed three 1 g subsamples of each soil sample and recorded the MIRS spectral response. Later, we calibrated and validated the recorded spectra using the OPUS v7.2 Spectroscopy Software and Partial Least Squares Regression (PLSR) model where the SLA dataset served as the calibration (70%) and validation (30%) data. We performed a log ratio transformation of the texture data to achieve a combined composition of 100% for sand%, silt%, and clay% after PLSR prediction. We used isometric log ratio transformation for this purpose (Niang et al., 2014). We used the 'compositions' package (van den Boogaart and Tolosana-Delgado, 2008) within the R software (version 3.3.2, R Core Team, 2018) for log transformation. Finally, we multiplied the SOC data by 1.72 to compute SOM.

### 2.3. Environmental covariates

A total of 14 environmental covariates were utilized for this study (Table 1). A 5 m spatial resolution digital elevation model (DEM) was created using the point elevation data ($n$ = 308) collected with the DGPS unit. We used the hydrologically correct DEM interpolation tool in ArcGIS 10.5 software for producing the DEM (Childs, 2004; Hutchinson, 1993). A group of topographic covariates was generated from this DEM using SAGA 2.1.2 software based on the work of Behrens et al. (2010), Lacoste et al. (2014), and Malone et al. (2009). The first and second derivatives, namely aspect, slope, multiresolution index of valley bottom flatness (MRVBF), multiresolution index of the ridge top flatness (MRRTF), positive and negative topographic openness, valley depth, terrain ruggedness index (TRI), total curvature, and total wetness index (TWI) were derived from the DEM.

In July 2016, an unmanned aerial vehicle (UAV) was flown over the study site to capture images in the visible bands (red-green-blue: RGB) of the electromagnetic spectrum. We used a DJI Matrice UAV which had a Zenmuse X3 CMOS sensor of 12.4 megapixels and 20 mm focal length. The flight altitude was 30 m above ground level capturing images of 2 cm spatial resolution. We processed the images and resampled to derive two covariates at 5 m resolution from this RGB imagery – the green band reflectance was used directly and another covariate (averaged RGB band reflectance) was generated by averaging the reflectance of the three bands for each pixel (Amini et al., 2005; Levin et al., 2005). These two covariates were selected to utilize the variation in soil and vegetation color. The historic polygon-based soil map, developed in 1981 and comprised of only 3 soil classes (Luttmerding, 1981), was used to derive a raster layer of clay content at 5 m resolution to use as an additional covariate. The polygon map consisted of single-component map units for our study site. We extracted values from the polygon soil map using the 40 × 40 m sampling grid and then, utilized Inverse Distance Weighting (IDW) interpolation to produce a raster surface.


**Fig. 2.** Location of the study site (49.08 N, 123.06 W) showing the standard laboratory analysis (SLA, $n = 62$) and mid-infrared spectroscopy (MIRS, $n = 308$) sample points following a 40 × 40 m grid. The SLA samples were also analyzed with MIRS.

**Table 1**
Environmental covariates used for digital soil mapping in this study.

| Environmental covariate type | Input representative data | Source data |
|---|---|---|
| Terrain | Digital elevation model (DEM) | Digital Elevation Model |
| | Aspect | |
| | Slope | |
| | Multiresolution index of valley bottom flatness (MRVBF) | |
| | Multiresolution index of the ridge top flatness (MRRTF) | |
| | Positive topographic openness | |
| | Negative topographic openness | |
| | Valley depth | |
| | Terrain ruggedness index (TRI) | |
| | Total curvature | |
| | Total wetness index (TWI) | |
| Vegetation & management | Green band reflectance | Unmanned aerial vehicle image |
| | Averaged RGB band reflectance | |
| Soil type | Clay raster surface | Historic soil map |

**Table 2**
Number of samples and total cost of various equivalent sampling efforts of standard laboratory analysis (SLA) and mid-infrared spectroscopy (MIRS).

| Sampling effort | Number of SLA samples | Number of SLA samples/ha | Number of MIRS samples | Number of MIRS samples/ha | Total cost (C$) |
|---|---|---|---|---|---|
| 100% | 62 | 1.15 | 308 | 5.70 | 2464 |
| 90% | 56 | 1.04 | 277 | 5.13 | 2216 |
| 80% | 50 | 0.93 | 246 | 4.56 | 1968 |
| 70% | 43 | 0.80 | 216 | 4.00 | 1728 |
| 60% | 37 | 0.69 | 185 | 3.43 | 1480 |
| 50% | 31 | 0.57 | 154 | 2.85 | 1232 |
| 40% | 25 | 0.46 | 123 | 2.28 | 984 |
| 30% | 19 | 0.35 | 92 | 1.70 | 736 |
| 20% | 12 | 0.22 | 62 | 1.15 | 496 |
| 10% | 6 | 0.11 | 31 | 0.57 | 248 |

### 2.4. Sampling efforts and conditioned Latin hypercube sampling

We used the Conditioned Latin Hypercube Sampling (cLHS) technique to develop several sampling efforts for both MIRS ($n$ = 308) and SLA ($n$ = 62) datasets using 10–90% of the total data points in 10% increments (Table 2). cLHS is a stratified random sampling technique that selects locations representing the spatial variability of the multiple input environmental covariates (Minasny and McBratney, 2006). The 'clhs' package (Roudier, 2014) within the R software (version 3.3.2, R Core Team, 2018) was used to design all sampling efforts. We utilized the environmental covariates listed in Table 1 for cLHS analysis. Sampling and analysis costs of each soil sample for both SLA and MIRS analyses were determined based on the cost of the external laboratory analyses, labor, and materials. The costs for SLA analyses, including the field sampling, was ~40C$/sample whereas the cost of MIRS analysis including the field sampling was ~8C$/sample. All laboratory fees are expressed on a cost-recovery basis.

### 2.5. Prediction and mapping

We used kriging with external drift (KED) to scale from point data to a continuous map of the entire field. The prediction using KED is based on the spatial correlation between the data points as well as the spatial information derived by the auxiliary environmental variables. As the name suggests, the drift is defined externally by the environmental variables rather than as a function of the coordinates of the data points (Wackernagel, 2003). In KED, prediction at an unknown location is derived by the following equation (Hengl, 2007):

$$\hat{z}(s_0) = \sum_{1=1}^{n} w_i(s_0) \cdot z(s_i) \quad (1)$$

for

$$\sum_{1=1}^{n} w_i(s_0) \cdot q_k(s_i) = q_k(s_0);\ k = 1, 2, \ldots\ldots, p \quad (2)$$

where $\hat{z}(s_0)$ is the target soil property predicted at location $s_0$, $q_k$'s are the environmental covariates, p is the number of environmental covariates. For kriging, it is critical to determine the spatial autocorrelation of the input data, i.e. semivariance which increases with distance. The distance where it stabilizes within the study area extent determines the range of the spatial autocorrelation (Malone et al., 2013). We used the 'gstat' package for R software (Pebesma and Heuvelink, 2016) to perform KED interpolations. The KED model used the environmental covariates listed in Table 1. However, we performed a Pearson correlation analysis to evaluate the relationship between the target soil property and the environmental covariates. Then, in KED prediction, we only included the variables which are highly correlated ($r \geq 0.20$ or $r \leq -0.20$) with the target soil property. For example, sand content of the soil appeared to have meaningful correlation with averaged RGB band reflectance ($r = 0.21$), clay raster surface ($r = -0.46$), DEM ($r = -0.22$), MRRTF ($r = 0.54$), MRVBF ($r = -0.43$), and valley depth ($r = -0.26$). Thus, we only included these six variables in the KED model for predicting the sand content.

### 2.6. Training and testing of the prediction models

We built and assessed the KED models separately for all the sampling efforts derived from the SLA and MIRS datasets. We randomly separated 25% ($n$ = 16) samples from the '100% sampling effort' of SLA dataset and utilized them for independent validation of all 20 models. Given the small sample size of the validation data set, this was repeated five times using a new set of randomly selected validation data for each iteration. We then reported the mean and standard deviation of the accuracy metrics for the five iterations.

We used four error indices for measuring the model performance: (i) the coefficient of determination ($R^2$); (ii) the Lin's concordance correlation coefficient (CCC); (iii) the root mean square error (RMSE); and (iv) the normalized root-mean-square error (nRMSE), where RMSE is normalized by dividing by the range of the observed data (Shen et al., 2016).

## 3. Results and discussion

### 3.1. Summary of soil properties and prediction using MIRS

There was considerable variability in different soil properties across the study site (Table 3). The soil was dominated by silt and relatively high clay content. The soil pH was within the optimum tolerance range of the cultivated crops, but the soil salinity (determined by EC) was relatively high. While the mean EC values below the 4 dS/m threshold were identified for crop production in this region (Bertrand, 1991), EC values determined in our study were as high as 16.9 dS/m The SOM and

**Table 3**
Summary statistics for soil sand, silt, clay, pH, electrical conductivity (EC), soil organic matter (SOM), and total nitrogen (TN) from the 0–15 cm depth for standard laboratory analysis (SLA) and mid-infrared spectroscopy (MIRS). CV refers to the coefficient of variation. The MIRS prediction accuracy derived from the SLA using partial least square regression is illustrated by the coefficient of determination ($R^2$) and root mean square error (RMSE).

| Soil property | SLA analyzed samples ($n$ = 62) | | | MIRS analyzed samples ($n$ = 308) | | | MIRS prediction accuracy | |
|---|---|---|---|---|---|---|---|---|
| | Mean | CV | Skewness | Mean | CV | Skewness | MIRS - $R^2$ | MIRS - RMSE |
| Sand (%) | 33.2 | 0.37 | 0.02 | 37.1 | 0.31 | 0.25 | 0.79 | 8.43 |
| Silt (%) | 50.4 | 0.19 | 0.08 | 47.6 | 0.20 | −0.01 | 0.78 | 6.57 |
| Clay (%) | 16.4 | 0.27 | 0.73 | 15.1 | 0.26 | 0.85 | 0.78 | 2.72 |
| pH | 5.5 | 0.05 | 0.52 | 5.6 | 0.05 | 0.39 | 0.71 | 0.42 |
| EC (dS/m) | 2.23 | 1.07 | 2.02 | 5.05 | 0.72 | 0.69 | 0.69 | 3.13 |
| SOM (%) | 5.4 | 0.20 | −1.07 | 5.1 | 0.18 | −1.02 | 0.87 | 0.46 |
| TN (%) | 0.28 | 0.21 | −0.91 | 0.26 | 0.19 | −0.61 | 0.88 | 0.04 |

TN were with the optimum ranges for vegetable production.

The skewness of the data indicated close to a normal distribution for most of the soil properties, with the exception of EC. Kriging interpolation, in general, does not perform well for highly skewed data (Ouyang et al., 2003) and thus, normality transformations were performed if data became highly skewed with different cLHS selections of sampling efforts.

Models derived from SLA and MIRS spectra using the PLSR were fairly accuracy for some soil properties, but not all (Table 3) highlighting the difference between SLA and MIRS data. The best predictions were attained for SOM and TN with $R^2$ values nearing 90%, while the pH and EC were predicted with lower accuracies ($R^2$ around 70%). Prediction accuracies for sand, silt, and clay were intermediate with $R^2$ values of nearly 80% and fell within or close to the range of $R^2$ values reported by other studies using MIRS and PLSR. For example, Masserschmidt et al. (1999) achieved $R^2$ of > 90% for SOM and Janik and Skjemstad (1995) reported an $R^2$ of 88% for N. Our findings were consistent with others who reported, consistently lower prediction accuracies for pH and EC. Janik et al. (1998) predicted EC with an $R^2$ of 23%, while Janik and Skjemstad (1995) found $R^2$ of 72% for predicting pH using the same techniques. In addition, Janik et al. (1998) predicted sand, silt, and clay with an $R^2$ of 88%, which is close to the accuracy we achieved in our study. While the reduction in accuracy due to modeling MIRS spectra is clear, particularly for some soil properties (i.e. up to 30% reduction), the cost savings for the differences in accuracy are large. In the present study, MIRS enabled about 5 times the amount of sampling for an equivalent cost.

### 3.2. Semivariogram – the analysis of spatial autocorrelation

The semivariogram analysis was used to compute the experimental variograms (EV), which identified the spatial structure of the data to be used for prediction. It was observed that the spatial structure weakens with decreasing sampling efforts (e.g. from 60% to 20% sampling effort). At the minimum sampling efforts (i.e. 10%, 20%, and 30%) there were limited to no spatial patterns, even after short separation distances, especially for the variograms of the SLA dataset.

As the spatial structure of the data changed with varying sampling efforts, the shape and structure of the EVs also differed. It was evident that the variograms were considerably different from each other for the varying intensities of sampling effort, with clear differences between the 60–100% and 20–40% sampling efforts. An example of how the EVs differed for various sampling efforts of the MIRS for TN is shown in Fig. 3. The maximum range of spatial autocorrelation was observed at the 100% sampling effort as 300 m. The range remained close to 300 m with the decreasing sampling intensities until it reached 60% sampling effort but subsequently, the range declined significantly. Moreover, the nugget effect representing the measurement errors or microscale variation causing a discontinuity in the EV near the origin (0,0) becomes larger with decreasing sample efforts. The higher nugget effect may result from the sparse sample distribution at the decreased sampling effort and consequent decline in spatial autocorrelation (Robinson and Metternicht, 2006). The decline of the spatial structure can be further realized if the nugget-to-sill ratios (N/S) are compared where N/S < 0.25 indicates strong spatial dependence and N/S ranging between 0.25 and 0.75 refers to moderate spatial dependence, and finally, N/S > 0.75 represents weak spatial dependence indicating poor or meaningless kriging prediction (Cambardella et al., 1994; Duffera et al., 2007). For the example demonstrated in Fig. 3, the N/S ratio ranged between 0.25 and 0.49 for the sampling efforts of 60% to 100%, indicating strong to moderate spatial dependence. However, at 40% sampling effort, the ratio declined to 0.81, which refers to poor spatial dependence, and at 20% sampling effort there was no spatial autocorrelation as observed by the level straight line of EV (Liu et al., 2006). Similar results were observed for the other soil properties for which 50% to 60% sampling efforts were found as the optimum mark after which the spatial autocorrelation declined substantially.

We also observed that the variance decreased or flattened out with the increasing lag distance and thus, at some reduced sampling efforts, EV could not be constructed (Kerry and Oliver, 2007). In the case of SLA sampling efforts, which comprise 80% fewer samples than its MIRS counterpart, poor spatial autocorrelation and variograms were detected even at higher sampling efforts. Fig. 4 displays examples of DSM for the study field at 5 m resolution of sand% and organic carbon% produced with SLA and MIRS datasets at 60% sampling effort. DSMs produced with MIRS dataset provided a more detailed representation of the surface compared to the DSMs produced with SLA dataset. MIRS DSMs showed clearly different patterns of soil property distribution than the SLA DSMs. In the MIRS DSMs, a greater range of values was predicted and there were fewer fine scale isolated patches of distinct values compared to the SLA DSMs. We also observed higher kriging prediction variance and edge effects for the SLA DSMs. Some linear features that were exhibited in the maps represent wide drainage ditches separating different field plots or the farm access roads.

### 3.3. Assessment of model performance

#### 3.3.1. Comparing equivalent sampling efforts of SLA and MIRS

When comparing the SLA and MIRS sampling efforts for predicting the digital soil maps, our analysis showed that the pattern of prediction accuracy differed widely across the soil properties and there was a clear difference in performance between SLA and MIRS (Figs. 5 and 6). It was

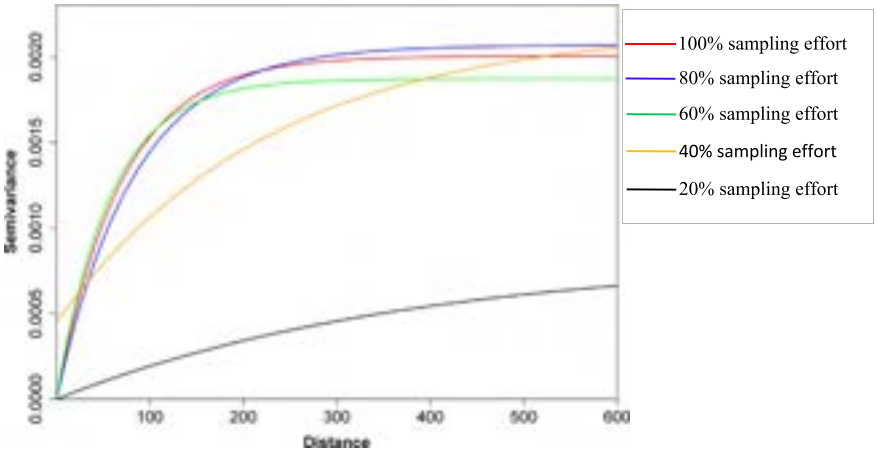


**Fig. 3.** Experimental semivariograms of total soil nitrogen data obtained by mid-infrared spectroscopy (MIRS) at different sampling efforts predicted using kriging with external drift model.

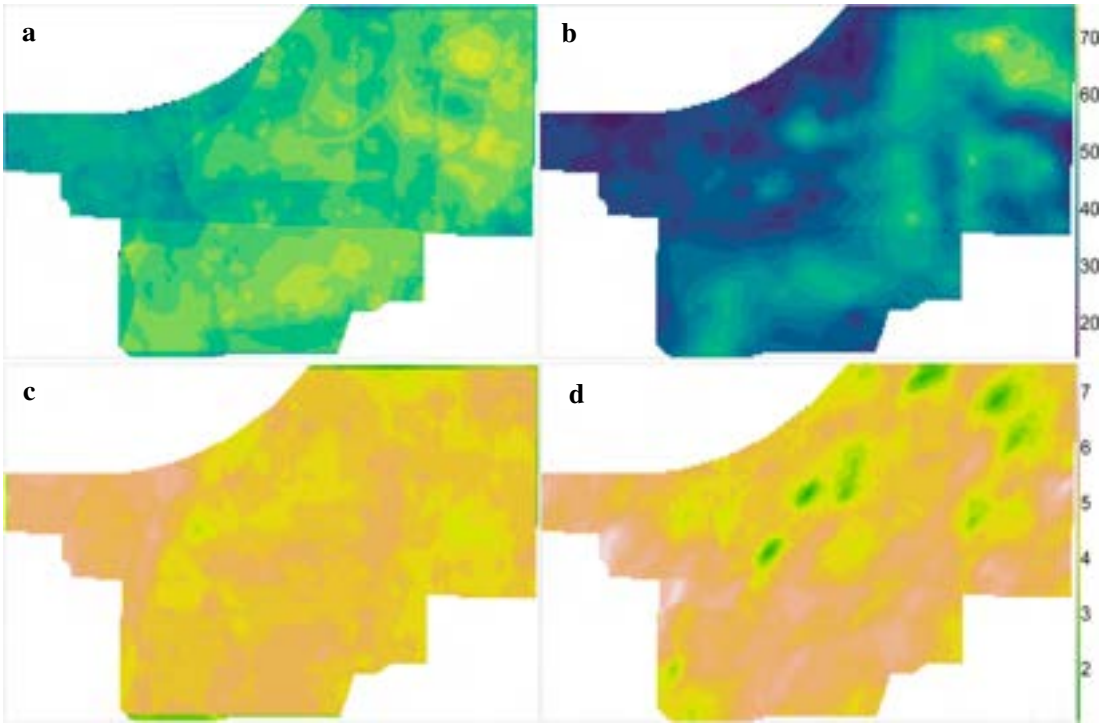


**Fig. 4.** Examples of digital soil maps for the study field at 5 m resolution of sand% produced with (a) standard laboratory analysis (SLA) or (b) mid-infrared spectroscopy (MIRS) and organic carbon% (c) with SLA or (d) with MIRS.

evident that MIRS always performed better than SLA at an equivalent sampling effort but the differences in accuracy decreased as the sampling efforts got smaller. For example, the difference in $R^2$ of sand prediction ranged from 0.45 to 0.52 for the 40% to 100% sampling efforts of SLA and MIRS while the difference was as low as 0.14 for < 40% sampling efforts. We also observed that accuracy measures, i.e. $R^2$, CCC, and nRMSE were not always in agreement when SLA and MIRS were compared for a specific model. In terms of $R^2$, the pH model for the MIRS dataset at 100% sampling effort, for instance, was 69% better than the output using the SLA dataset. However, the same prediction output was only 35% and 18% better when nRMSE and CCC values, respectively, were compared. Despite the lower lab accuracy as explained in Section 3.1, the overall performance of the MIRS dataset was substantially better than that of the SLA dataset for each equivalent sampling effort. In our analysis, the MIRS dataset had about 5 times more samples than its SLA counterpart for the same cost, thus capturing more of the spatial variability across the study site and producing stronger prediction performances. If equivalent sampling densities (i.e. number of samples), however, were compared instead of the sampling efforts, we might obtain different results. For example, both SLA-100% and MIRS-20% sampling efforts had a total of 62 samples and from the results, it was clear that SLA-100% performed better than MIRS-20% sampling efforts for all the soil properties. This might be due to the prediction inaccuracies occurred during producing the MIRS dataset as explained in Section 3.1. Yet, our analysis illustrated that the spatial variability was not effectively captured with such a small number of samples (i.e. $n = 62$), resulting in weak prediction performances.

Our findings are similar to several previous studies that also confirmed that the use of the MIRS technique allowed them to utilize more sample points for DSM and the additional points helped them acquire better prediction accuracies without increasing the cost of analysis. A recent regional-scale study conducted in south-west Germany, using MIRS and kriging interpolation, generated SOM map with high accuracy as indicated by the overall similarity of 48–69% with the existing digital map (Mirzaeitalarposhti et al. 2017). Mirzaeitalarposhti et al. (2017) also concluded that the use of MIRS significantly reduced the cost of their research as 90% of the samples were analyzed with the MIRS technique although no cost comparison with SLA was provided. Another study by World Agroforestry Center reported that MIRS analysis of SOC data reduced the cost by 70% as compared to that of traditional chemical analysis in their African soil information project (Nocita et al., 2015). O'Rourke and Holden (2011) found spectroscopic analysis was 10 times more cost effective than SLA. In our analysis, the MIRS dataset was 5 times more cost effective than the SLA dataset. The low cost for MIRS enabled the use of far more data points than SLA for DSM for an equivalent sampling effort, clearly resulting in better prediction accuracies for all the soil properties.

### 3.3.2. *Trade-offs between cost and accuracy of the predictive models*

The results of the model assessment described above clearly show that the relationship between sampling efforts and prediction accuracy was generally non-linear for most of the soil properties (Figs. 5 and 6). With decreasing sampling efforts, the prediction accuracy declined exponentially for most soil properties regardless of methodology or accuracy metric. In a few cases, the decline was sharper and more linear, e.g. the decline in CCC of silt prediction between 50% and 20% of SLA sampling efforts (Fig. 5), and the decline in $R^2$ of pH prediction between 50% and 10% of MIRS sampling efforts (Fig. 6).

We found that the prediction accuracies significantly improved up to the 50% to 60% sampling efforts of both SLA and MIRS and after this point, the accuracy did not equally improve. Similar results were obtained by Simbahan and Dobermann (2006) when they tested the prediction accuracy of a regression kriging model for SOC using sample sizes of 50, 100, 150, and 200 and found that RMSE of prediction did not improve or minimally improved after reaching the sample size of 100. However, as we already mentioned, predictions using the MIRS datasets were more accurate than the predictions using the SLA datasets at equivalent sampling efforts. While data points were added with the increasing sampling efforts, the spatial autocorrelation was captured at the 50% to 60% sampling effort, which resulted in the most effective prediction performance in terms of both the prediction accuracy and cost. For example, the CCC values of sand prediction using the MIRS

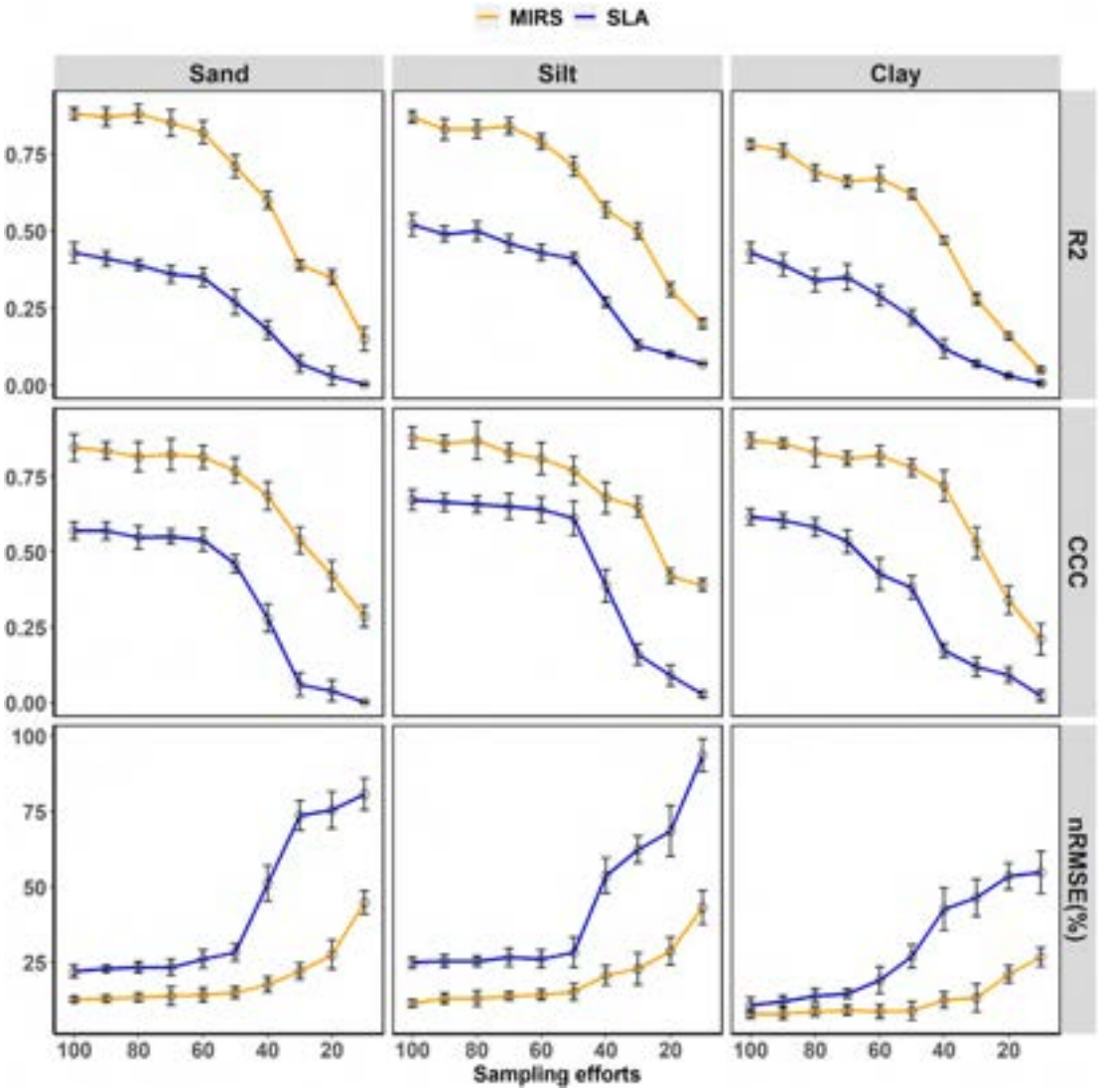


**Fig. 5.** Model assessment of the prediction of sand, silt, and clay at various equivalent sampling efforts of standard laboratory analysis (SLA) and mid-infrared spectroscopy (MIRS) datasets using kriging with external drift. Means and standard deviation (error bars) of the iterative analysis of coefficient of determination ($R^2$), Lin's concordance correlation coefficient (CCC), and normalized root mean square error (nRMSE) are shown.

dataset were improved by 184% between 10% and 60% sampling efforts, whereas between 60% and 100% sampling efforts accuracy only improved by 4%. This 4% improvement in accuracy for CCC between the 60% and 100% sampling efforts cost 984C$; i.e. 246C$/1% accuracy improvement. In contrast, an investment of only 7C$/1% accuracy improvement of CCC was required between 10% and 60% sapling efforts. For a dynamic soil property such as pH, the prediction using MIRS dataset required an investment of 4C$/1% improvement of CCC between 10% and 50% sampling efforts, whereas the investment was 93C$/1% improvement between 50% and 100% sampling efforts. Mapping using the full dataset of 308 points with SLA would have cost 12,320C$, whereas the total cost of full MIRS dataset was only 2464C$, highlighting the cost efficiency of using the MIRS technique. Although the investment for 1% accuracy improvement varies for different soil properties, it was clear that the model performance was most cost-effective at the 50% to 60% sampling efforts considering the high incremental cost and the unequal gain in the prediction accuracy above 60%.

Thus, applying the cLHS sample selection technique and sampling at an intensity of 2–3 samples per hectare (i.e. 50–60% data points of the initial sampling effort derived from a 40 × 40 m grid) provided the most effective sample design for DSM for our study field in terms of the accuracy of the KED model and costs. This sampling density is substantially different than that determined by Kerry et al. (2010) for a study field in Wallingford, England. Using a 30 × 30 m sampling grid for their analysis, they reported that spatial variability was captured most effectively at the 100–120 m sampling interval (i.e. 0.7–1 sample per hectare). Although our sampling intensity was higher than in Wallingford, this may not be the most effective intensity in all cases as soil property, environmental conditions, and management strategy vary from site to site. While it is unlikely that farmers would sample at such high density by hand frequently, our analysis demonstrates the intensity of sampling that could be employed to calibrate hand-held or tractor mounted MIRS techniques.

## 4. Conclusions

Identifying an effective sampling effort is critical for maximizing the accuracy and minimizing the cost of DSM models. We compared 20 different sampling efforts derived from the datasets of standard laboratory analysis (SLA) and mid-infrared spectroscopy (MIRS) for producing digital maps of a suite of soil properties including sand, silt, clay, pH, EC, SOM and TN. We determined that at an equivalent sampling effort the MIRS dataset produced more accurate maps of selected

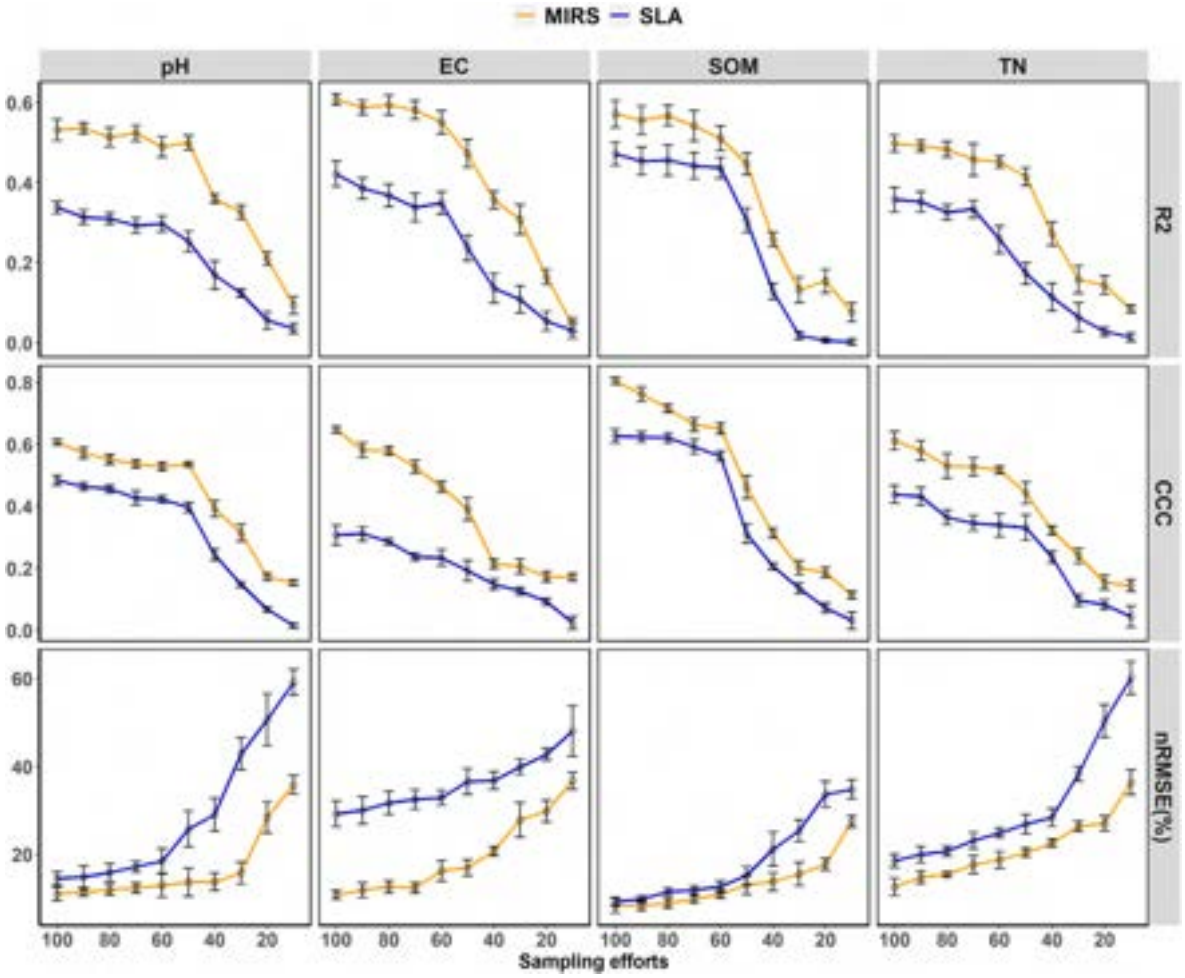


**Fig. 6.** Model assessment of the prediction of soil pH, electrical conductivity (EC), soil organic matter (SOM) and total nitrogen (TN) at various sampling efforts of standard laboratory analysis (SLA) and mid-infrared spectroscopy (MIRS) datasets using kriging with external drift. Means and standard deviation (error bars) of the iterative analysis of the coefficient of determination ($R^2$), Lin's concordance correlation coefficient (CCC), and normalized root mean square error (nRMSE) are shown.

soil properties as compared to the maps predicted by SLA datasets, although the prediction accuracy varied across the soil properties and by accuracy metric (e.g. $R^2$, CCC, and nRMSE). Our analysis showed that the cost per improvement in accuracy with increasing sampling efforts was optimized at the 50–60% sampling effort. Thus, a sampling density of 2–3 samples per hectare, selected using a spatial sample selection technique (e.g. cLHS), and analyzed using MIRS in the lab was the most cost effective approach for the production of accurate DSMs for our study field. However, these findings may vary for mapping in other crop fields with different soils, topography or management history. Hence, further analysis should explore how these findings may differ based on soil type, environmental covariates, or field management.

## Acknowledgments

We would like to acknowledge the funding support from the Farm Adaptation Innovator Program of the British Columbia Climate Action Initiative. We also thank the producer for access to his field for sampling purposes.

## Appendix 1

| Sampling efforts | Soil property | Metrics | SLA | SLA SD | MIRS | MIRS SD | Metrics | SLA | SLA SD | MIRS | MIRS SD | Metrics (%) | SLA | SLA SD | MIRS | MIRS.SD |
|---|---|---|---|---|---|---|---|---|---|---|---|---|---|---|---|---|
| 100% | Sand | $R^2$ | 0.430 | 0.033 | 0.880 | 0.020 | CCC | 0.570 | 0.029 | 0.847 | 0.044 | nRMSE | 22.048 | 2.119 | 12.771 | 0.753 |
| 90% | Sand | $R^2$ | 0.410 | 0.024 | 0.870 | 0.030 | CCC | 0.570 | 0.029 | 0.836 | 0.029 | nRMSE | 22.849 | 1.130 | 12.909 | 1.221 |
| 80% | Sand | $R^2$ | 0.390 | 0.018 | 0.880 | 0.030 | CCC | 0.548 | 0.038 | 0.816 | 0.049 | nRMSE | 23.334 | 1.849 | 13.316 | 1.470 |
| 70% | Sand | $R^2$ | 0.360 | 0.028 | 0.850 | 0.042 | CCC | 0.551 | 0.025 | 0.823 | 0.052 | nRMSE | 23.261 | 2.735 | 13.870 | 3.053 |
| 60% | Sand | $R^2$ | 0.350 | 0.030 | 0.820 | 0.036 | CCC | 0.540 | 0.037 | 0.815 | 0.038 | nRMSE | 26.040 | 3.094 | 14.173 | 2.283 |
| 50% | Sand | $R^2$ | 0.270 | 0.040 | 0.710 | 0.036 | CCC | 0.460 | 0.030 | 0.770 | 0.042 | nRMSE | 28.271 | 2.873 | 14.937 | 1.912 |
| 40% | Sand | $R^2$ | 0.180 | 0.030 | 0.600 | 0.028 | CCC | 0.280 | 0.046 | 0.686 | 0.047 | nRMSE | 51.125 | 5.923 | 17.615 | 2.568 |
| 30% | Sand | $R^2$ | 0.070 | 0.029 | 0.390 | 0.016 | CCC | 0.060 | 0.038 | 0.538 | 0.044 | nRMSE | 73.630 | 4.892 | 22.077 | 2.739 |
| 20% | Sand | $R^2$ | 0.030 | 0.030 | 0.350 | 0.025 | CCC | 0.039 | 0.035 | 0.422 | 0.049 | nRMSE | 75.411 | 6.138 | 27.530 | 4.836 |
| 10% | Sand | $R^2$ | 0.004 | 0.003 | 0.150 | 0.038 | CCC | 0.002 | 0.002 | 0.286 | 0.036 | nRMSE | 80.693 | 5.302 | 44.801 | 3.882 |
| 100% | Silt | $R^2$ | 0.520 | 0.037 | 0.870 | 0.020 | CCC | 0.673 | 0.034 | 0.880 | 0.035 | nRMSE | 24.903 | 1.857 | 11.392 | 1.220 |

| | | | | | | | | | | | | | | | | |
|---|---|---|---|---|---|---|---|---|---|---|---|---|---|---|---|---|
| 90% | Silt | $R^2$ | 0.490 | 0.026 | 0.830 | 0.034 | CCC | 0.665 | 0.030 | 0.860 | 0.027 | nRMSE | 25.432 | 2.119 | 13.037 | 1.813 |
| 80% | Silt | $R^2$ | 0.500 | 0.031 | 0.830 | 0.029 | CCC | 0.658 | 0.028 | 0.870 | 0.062 | nRMSE | 25.318 | 1.733 | 12.974 | 2.514 |
| 70% | Silt | $R^2$ | 0.460 | 0.028 | 0.840 | 0.027 | CCC | 0.651 | 0.043 | 0.830 | 0.032 | nRMSE | 26.631 | 3.025 | 13.752 | 1.376 |
| 60% | Silt | $R^2$ | 0.430 | 0.027 | 0.790 | 0.025 | CCC | 0.641 | 0.041 | 0.810 | 0.053 | nRMSE | 26.089 | 3.017 | 14.253 | 1.791 |
| 50% | Silt | $R^2$ | 0.410 | 0.018 | 0.710 | 0.032 | CCC | 0.612 | 0.057 | 0.770 | 0.046 | nRMSE | 28.305 | 4.931 | 15.179 | 2.823 |
| 40% | Silt | $R^2$ | 0.270 | 0.017 | 0.570 | 0.025 | CCC | 0.388 | 0.054 | 0.680 | 0.052 | nRMSE | 53.701 | 5.923 | 20.623 | 3.247 |
| 30% | Silt | $R^2$ | 0.130 | 0.016 | 0.500 | 0.026 | CCC | 0.160 | 0.035 | 0.650 | 0.033 | nRMSE | 62.417 | 4.451 | 22.827 | 5.346 |
| 20% | Silt | $R^2$ | 0.100 | 0.008 | 0.310 | 0.023 | CCC | 0.090 | 0.034 | 0.420 | 0.025 | nRMSE | 68.532 | 8.378 | 28.661 | 4.581 |
| 10% | Silt | $R^2$ | 0.070 | 0.002 | 0.200 | 0.017 | CCC | 0.028 | 0.011 | 0.390 | 0.021 | nRMSE | 93.572 | 5.404 | 43.172 | 5.591 |
| 100% | Clay | $R^2$ | 0.430 | 0.033 | 0.780 | 0.017 | CCC | 0.617 | 0.027 | 0.870 | 0.024 | nRMSE | 10.783 | 2.547 | 7.832 | 1.512 |
| 90% | Clay | $R^2$ | 0.390 | 0.037 | 0.760 | 0.023 | CCC | 0.604 | 0.025 | 0.860 | 0.016 | nRMSE | 11.935 | 2.059 | 8.015 | 2.063 |
| 80% | Clay | $R^2$ | 0.340 | 0.036 | 0.690 | 0.026 | CCC | 0.582 | 0.030 | 0.830 | 0.047 | nRMSE | 13.831 | 2.392 | 8.573 | 1.462 |
| 70% | Clay | $R^2$ | 0.350 | 0.041 | 0.660 | 0.017 | CCC | 0.535 | 0.038 | 0.810 | 0.023 | nRMSE | 14.552 | 1.586 | 9.117 | 1.647 |
| 60% | Clay | $R^2$ | 0.290 | 0.033 | 0.670 | 0.039 | CCC | 0.427 | 0.053 | 0.820 | 0.033 | nRMSE | 19.085 | 4.373 | 8.714 | 2.308 |
| 50% | Clay | $R^2$ | 0.220 | 0.025 | 0.620 | 0.016 | CCC | 0.382 | 0.039 | 0.780 | 0.029 | nRMSE | 26.972 | 3.813 | 8.937 | 3.015 |
| 40% | Clay | $R^2$ | 0.120 | 0.031 | 0.470 | 0.013 | CCC | 0.173 | 0.024 | 0.720 | 0.051 | nRMSE | 42.584 | 7.004 | 12.470 | 2.672 |
| 30% | Clay | $R^2$ | 0.070 | 0.010 | 0.280 | 0.018 | CCC | 0.118 | 0.032 | 0.530 | 0.052 | nRMSE | 46.446 | 6.191 | 13.179 | 4.661 |
| 20% | Clay | $R^2$ | 0.030 | 0.006 | 0.160 | 0.010 | CCC | 0.091 | 0.026 | 0.340 | 0.047 | nRMSE | 53.504 | 4.338 | 21.017 | 2.803 |
| 10% | Clay | $R^2$ | 0.007 | 0.007 | 0.050 | 0.008 | CCC | 0.022 | 0.019 | 0.210 | 0.051 | nRMSE | 54.730 | 7.074 | 26.749 | 3.152 |
| 100% | pH | $R^2$ | 0.338 | 0.015 | 0.532 | 0.027 | CCC | 0.484 | 0.016 | 0.607 | 0.009 | nRMSE | 14.463 | 1.518 | 11.043 | 1.582 |
| 90% | pH | $R^2$ | 0.314 | 0.018 | 0.536 | 0.014 | CCC | 0.464 | 0.013 | 0.572 | 0.018 | nRMSE | 14.861 | 2.500 | 11.364 | 0.834 |
| 80% | pH | $R^2$ | 0.310 | 0.014 | 0.514 | 0.024 | CCC | 0.456 | 0.012 | 0.551 | 0.016 | nRMSE | 15.849 | 2.015 | 11.973 | 1.260 |
| 70% | pH | $R^2$ | 0.293 | 0.019 | 0.524 | 0.020 | CCC | 0.427 | 0.023 | 0.537 | 0.013 | nRMSE | 17.181 | 1.284 | 12.351 | 1.145 |
| 60% | pH | $R^2$ | 0.297 | 0.020 | 0.490 | 0.025 | CCC | 0.422 | 0.012 | 0.528 | 0.013 | nRMSE | 18.447 | 2.887 | 12.947 | 2.731 |
| 50% | pH | $R^2$ | 0.253 | 0.026 | 0.500 | 0.018 | CCC | 0.397 | 0.016 | 0.536 | 0.007 | nRMSE | 25.768 | 4.092 | 13.628 | 3.203 |
| 40% | pH | $R^2$ | 0.169 | 0.035 | 0.360 | 0.011 | CCC | 0.243 | 0.018 | 0.392 | 0.026 | nRMSE | 29.058 | 3.739 | 13.774 | 2.005 |
| 30% | pH | $R^2$ | 0.124 | 0.010 | 0.326 | 0.017 | CCC | 0.147 | 0.008 | 0.314 | 0.027 | nRMSE | 42.869 | 3.681 | 15.735 | 2.525 |
| 20% | pH | $R^2$ | 0.056 | 0.022 | 0.210 | 0.017 | CCC | 0.067 | 0.007 | 0.172 | 0.012 | nRMSE | 50.630 | 5.945 | 28.436 | 3.568 |
| 10% | pH | $R^2$ | 0.036 | 0.013 | 0.094 | 0.022 | CCC | 0.015 | 0.008 | 0.153 | 0.009 | nRMSE | 59.151 | 2.919 | 35.843 | 2.093 |
| 100% | EC | $R^2$ | 0.422 | 0.032 | 0.608 | 0.014 | CCC | 0.307 | 0.032 | 0.647 | 0.011 | nRMSE | 29.194 | 2.907 | 10.751 | 1.020 |
| 90% | EC | $R^2$ | 0.386 | 0.026 | 0.588 | 0.018 | CCC | 0.311 | 0.023 | 0.582 | 0.024 | nRMSE | 30.010 | 3.130 | 11.851 | 1.694 |
| 80% | EC | $R^2$ | 0.368 | 0.028 | 0.594 | 0.025 | CCC | 0.286 | 0.011 | 0.579 | 0.014 | nRMSE | 31.665 | 2.629 | 12.594 | 1.379 |
| 70% | EC | $R^2$ | 0.338 | 0.035 | 0.582 | 0.023 | CCC | 0.237 | 0.012 | 0.527 | 0.021 | nRMSE | 32.477 | 2.215 | 12.392 | 1.173 |
| 60% | EC | $R^2$ | 0.349 | 0.028 | 0.551 | 0.029 | CCC | 0.234 | 0.026 | 0.463 | 0.018 | nRMSE | 32.870 | 1.738 | 16.220 | 2.335 |
| 50% | EC | $R^2$ | 0.237 | 0.032 | 0.473 | 0.035 | CCC | 0.192 | 0.033 | 0.391 | 0.037 | nRMSE | 36.560 | 2.931 | 16.951 | 1.852 |
| 40% | EC | $R^2$ | 0.136 | 0.037 | 0.357 | 0.022 | CCC | 0.148 | 0.017 | 0.214 | 0.015 | nRMSE | 36.780 | 2.039 | 20.732 | 1.074 |
| 30% | EC | $R^2$ | 0.108 | 0.034 | 0.308 | 0.037 | CCC | 0.126 | 0.012 | 0.206 | 0.023 | nRMSE | 39.905 | 1.771 | 27.822 | 3.960 |
| 20% | EC | $R^2$ | 0.054 | 0.024 | 0.164 | 0.019 | CCC | 0.092 | 0.012 | 0.173 | 0.017 | nRMSE | 42.757 | 1.415 | 29.833 | 2.476 |
| 10% | EC | $R^2$ | 0.031 | 0.020 | 0.044 | 0.019 | CCC | 0.024 | 0.020 | 0.171 | 0.012 | nRMSE | 48.091 | 5.755 | 36.701 | 1.965 |
| 100% | SOM | $R^2$ | 0.472 | 0.029 | 0.572 | 0.034 | CCC | 0.627 | 0.022 | 0.804 | 0.011 | nRMSE | 9.233 | 0.992 | 8.371 | 1.663 |
| 90% | SOM | $R^2$ | 0.454 | 0.035 | 0.556 | 0.036 | CCC | 0.624 | 0.017 | 0.762 | 0.024 | nRMSE | 9.815 | 0.752 | 8.299 | 1.105 |
| 80% | SOM | $R^2$ | 0.456 | 0.038 | 0.568 | 0.025 | CCC | 0.621 | 0.016 | 0.716 | 0.014 | nRMSE | 11.458 | 0.846 | 8.861 | 1.048 |
| 70% | SOM | $R^2$ | 0.442 | 0.033 | 0.542 | 0.038 | CCC | 0.592 | 0.023 | 0.663 | 0.021 | nRMSE | 11.828 | 0.959 | 9.829 | 0.902 |
| 60% | SOM | $R^2$ | 0.437 | 0.026 | 0.511 | 0.031 | CCC | 0.562 | 0.016 | 0.651 | 0.018 | nRMSE | 12.676 | 1.311 | 10.884 | 0.893 |
| 50% | SOM | $R^2$ | 0.306 | 0.031 | 0.447 | 0.027 | CCC | 0.311 | 0.031 | 0.462 | 0.037 | nRMSE | 15.168 | 2.017 | 13.034 | 2.117 |
| 40% | SOM | $R^2$ | 0.128 | 0.021 | 0.258 | 0.018 | CCC | 0.206 | 0.011 | 0.313 | 0.015 | nRMSE | 21.209 | 3.894 | 13.790 | 2.067 |
| 30% | SOM | $R^2$ | 0.018 | 0.010 | 0.132 | 0.032 | CCC | 0.136 | 0.018 | 0.201 | 0.023 | nRMSE | 25.385 | 2.504 | 15.480 | 2.671 |
| 20% | SOM | $R^2$ | 0.006 | 0.005 | 0.154 | 0.029 | CCC | 0.072 | 0.016 | 0.187 | 0.017 | nRMSE | 33.633 | 2.900 | 17.713 | 1.332 |
| 10% | SOM | $R^2$ | 0.002 | 0.008 | 0.076 | 0.023 | CCC | 0.031 | 0.027 | 0.113 | 0.012 | nRMSE | 34.781 | 2.143 | 27.480 | 1.255 |
| 100% | TN | $R^2$ | 0.358 | 0.031 | 0.498 | 0.021 | CCC | 0.438 | 0.029 | 0.612 | 0.030 | nRMSE | 18.547 | 1.499 | 12.564 | 1.980 |
| 90% | TN | $R^2$ | 0.352 | 0.025 | 0.492 | 0.014 | CCC | 0.432 | 0.029 | 0.580 | 0.032 | nRMSE | 19.952 | 1.824 | 14.805 | 1.419 |
| 80% | TN | $R^2$ | 0.326 | 0.019 | 0.484 | 0.019 | CCC | 0.364 | 0.024 | 0.530 | 0.040 | nRMSE | 20.728 | 1.155 | 15.405 | 0.570 |
| 70% | TN | $R^2$ | 0.334 | 0.022 | 0.458 | 0.040 | CCC | 0.346 | 0.025 | 0.528 | 0.029 | nRMSE | 23.132 | 1.881 | 17.646 | 2.005 |
| 60% | TN | $R^2$ | 0.258 | 0.034 | 0.452 | 0.015 | CCC | 0.339 | 0.037 | 0.517 | 0.012 | nRMSE | 24.887 | 1.096 | 18.738 | 1.893 |
| 50% | TN | $R^2$ | 0.173 | 0.027 | 0.415 | 0.022 | CCC | 0.331 | 0.041 | 0.443 | 0.035 | nRMSE | 26.908 | 2.168 | 20.362 | 1.005 |
| 40% | TN | $R^2$ | 0.114 | 0.035 | 0.272 | 0.029 | CCC | 0.236 | 0.019 | 0.322 | 0.014 | nRMSE | 28.378 | 2.047 | 22.562 | 0.893 |
| 30% | TN | $R^2$ | 0.064 | 0.036 | 0.158 | 0.034 | CCC | 0.096 | 0.018 | 0.240 | 0.024 | nRMSE | 38.305 | 1.634 | 26.452 | 1.201 |
| 20% | TN | $R^2$ | 0.028 | 0.011 | 0.144 | 0.023 | CCC | 0.082 | 0.016 | 0.154 | 0.023 | nRMSE | 50.330 | 3.717 | 27.052 | 1.700 |
| 10% | TN | $R^2$ | 0.014 | 0.011 | 0.084 | 0.009 | CCC | 0.044 | 0.034 | 0.144 | 0.019 | nRMSE | 60.134 | 3.732 | 36.375 | 2.796 |

## References


Amini, M., Afyuni, M., Fathianpour, N., Khademi, H., Flühler, H., 2005. Continuous soil pollution mapping using fuzzy logic and spatial interpolation. Geoderma 124, 223–233.

Behrens, T., Zhu, A.X., Schmidt, K., Scholten, T., 2010. Multi-scale digital terrain analysis and feature selection for digital soil mapping. Geoderma 155, 175–185. https://doi.org/10.1016/j.geoderma.2009.07.010.

Bertrand, R., 1991. Soil Management Handbook for the Lower Fraser Valley, 2nd ed. B.C. Ministry of Agriculture, Fisheries and Food, Abbosford.

van den Boogaart, K.G., Tolosana-Delgado, R., 2008. "Compositions": a unified R package to analyze compositional data. Comput. Geosci. 34, 320–338.

Brungard, C., Boettinger, J., 2010. Conditioned latin hypercube sampling: optimal sample size for digital soil mapping of arid rangelands in Utah, USA. In: Digital Soil Mapping. Springer, Netherlands, pp. 67–75. https://doi.org/10.1007/978-90-481-8863-5_6.

Brus, D.J., Heuvelink, G.B.M., 2007. Optimization of sample patterns for universal kriging of environmental variables. Geoderma 138, 86–95.

Cambardella, C.A., Moorman, T.B., Parkin, T.B., Karlen, D.L., Novak, J.M., Turco, R.F., Konopka, A.E., 1994. Field-scale variability of soil properties in central Iowa soils. Soil Sci. Soc. Am. J. 58, 1501–1511.

Childs, C., 2004. Interpolating surfaces in ArcGIS spatial analyst. ArcUser 3235, 569 July-September.

Cobo, J., Dercon, G., Yekeye, T., Chapungu, L., Kadzere, C., Murwira, A., Delve, R., Cadisch, G., 2010. Integration of mid-infrared spectroscopy and geostatistics in the assessment of soil spatial variability at landscape level. 158, 398–411. https://doi.org/10.1016/j.geoderma.2010.06.013.

Cruz-Cárdenas, G., López-Mata, L., Ortiz-Solorio, C.A., Villaseñor, J.L., Ortiz, E., Silva, J.T., Estrada-Godoy, F., 2014. Interpolation of Mexican soil properties at a scale of 1:1,000,000. Geoderma 213, 29–35. https://doi.org/10.1016/j.geoderma.2013.07.014.

Duffera, M., White, J.G., Weisz, R., 2007. Spatial variability of Southeastern US Coastal Plain soil physical properties: implications for site-specific management. Geoderma 137, 327–339.

Environment Canada, 2019. Canadian climate Normals 1981-2010 [WWW document]. URL. http://climate.weather.gc.ca/climate_normals/results_1981_2010_e.html?searchType=stnName&txtStationName=delta&searchMethod=contains&txtCentralLatMin=0&txtCentralLatSec=0&txtCentralLongMin=0&

txtCentralLongSec=0&stnID=766&dispBack=0, Accessed date: 23 March 2019.
Ge, Y., Thomasson, J.A., Sui, R., 2011. Remote sensing of soil properties in precision agriculture: a review. Front. Earth Sci. 5, 229–238. https://doi.org/10.1007/s11707-011-0175-0.
Grunwald, S., Thompson, J.A., Boettinger, J.L., 2011. Digital soil mapping and modeling at continental scales: finding solutions for global issues. Soil Sci. Soc. Am. J. 75, 1201–1213.
Hengl, T., 2007. A practical guide to geostatistical mapping. Scientific and Technical Research series. https://doi.org/10.1016/0277-9390(86)90082-8.
Hengl, T., Heuvelink, G.B.M., Stein, A., 2004. A generic framework for spatial prediction of soil variables based on regression-kriging. Geoderma 120, 75–93. https://doi.org/10.1016/j.geoderma.2003.08.018.
Hutchinson, M.F., 1993. Development of a continent-wide DEM with applications to terrain and climate analysis. In: Goodchild, M.F. (Ed.), Environmental Modeling with GIS. Oxford University Press, New York, pp. 392–399.
Janik, L.J., Skjemstad, J.O., 1995. Characterization and analysis of soils using mid-infrared partial least-squares. 2. Correlations with some laboratory data. Soil Res 33, 637–650.
Janik, L.J., Merry, R.H., Skjemstad, J.O., 1998. Can mid infrared diffuse reflectance analysis replace soil extractions? Aust. J. Exp. Agric. 38, 681–696.
Kerry, R., Oliver, M.A., 2007. Comparing sampling needs for variograms of soil properties computed by the method of moments and residual maximum likelihood. Geoderma 140, 383–396.
Kerry, R., Oliver, M.A., Frogbrook, Z.L., 2010. Sampling in precision agriculture. In: Geostatistical Applications for Precision Agriculture. Springer, Dordrecht, pp. 35–63.
Keskin, H., Grunwald, S., 2018. Regression kriging as a workhorse in the digital soil mapper's toolbox. Geoderma 326, 22–41.
Lacoste, M., Minasny, B., McBratney, A., Michot, D., Viaud, V., Walter, C., 2014. High resolution 3D mapping of soil organic carbon in a heterogeneous agricultural landscape. Geoderma 213, 296–311. https://doi.org/10.1016/j.geoderma.2013.07.002.
Lagacherie, P., 2008. Digital soil mapping: A state of the art. In: Digital Soil Mapping with Limited Data. Springer Netherlands, Dordrecht, pp. 3–14. https://doi.org/10.1007/978-1-4020-8592-5_1.
Levin, N., Ben-Dor, E., Singer, A., 2005. A digital camera as a tool to measure colour indices and related properties of sandy soils in semi-arid environments. Int. J. Remote Sens. 26, 5475–5492.
Li, Y., 2010. Can the spatial prediction of soil organic matter contents at various sampling scales be improved by using regression kriging with auxiliary information? Geoderma 159, 63–75.
Li, J., Heap, A.D., 2011. A review of comparative studies of spatial interpolation methods in environmental sciences: performance and impact factors. Ecol. Inform. 6, 228–241. https://doi.org/10.1016/j.ecoinf.2010.12.003.
Li, H., Webster, R., Shi, Z., 2015. Mapping soil salinity in the Yangtze delta: REML and universal kriging (E-BLUP) revisited. Geoderma 237–238, 71–77. https://doi.org/10.1016/j.geoderma.2014.08.008.
Ließ, M., 2015. Sampling for regression-based digital soil mapping: closing the gap between statistical desires and operational applicability. Spat. Stat. 13, 106–122. https://doi.org/10.1016/j.spasta.2015.06.002.
Liu, D., Wang, Z., Zhang, B., Song, K., Li, X., Li, J., Li, F., Duan, H., 2006. Spatial distribution of soil organic carbon and analysis of related factors in croplands of the black soil region, Northeast China. Agric. Ecosyst. Environ. 113, 73–81.
Luttmerding, H., 1981. Soils of the Langley-Vancouver Map Area. Kelowna.
Malone, B.P., McBratney, A.B., Minasny, B., Laslett, G.M., 2009. Mapping continuous depth functions of soil carbon storage and available water capacity. Geoderma 154, 138–152. https://doi.org/10.1016/j.geoderma.2009.10.007.
Malone, B., McBratney, A., Minasny, B., 2013. Spatial scaling for digital soil mapping. Soil Sci. Soc. Am. J. 77, 890–902. https://doi.org/10.2136/sssaj2012.0419.
Malone, B.P., Styc, Q., Minasny, B., McBratney, A.B., 2017. Digital soil mapping of soil carbon at the farm scale: a spatial downscaling approach in consideration of measured and uncertain data. Geoderma 290, 91–99. https://doi.org/10.1016/J.GEODERMA.2016.12.008.
Masserschmidt, I., Cuelbas, C.J., Poppi, R.J., De Andrade, J.C., De Abreu, C.A., Davanzo, C.U., 1999. Determination of organic matter in soils by FTIR/diffuse reflectance and multivariate calibration. J. Chemom. 13, 265–273.
Minasny, B., McBratney, A.B., 2006. A conditioned Latin hypercube method for sampling in the presence of ancillary information. Comput. Geosci. 32, 1378–1388. https://doi.org/10.1016/j.cageo.2005.12.009.
Mirzaeitalarposhti, R., Demyan, M.S., Rasche, F., Cadisch, G., Müller, T., 2017. Mid-infrared spectroscopy to support regional-scale digital soil mapping on selected croplands of South-West Germany. Catena 149, 283–293.
Niang, M.A., Nolin, M.C., Jégo, G., Perron, I., 2014. Digital mapping of soil texture using RADARSAT-2 polarimetric synthetic aperture radar data. Soil Sci. Soc. Am. J. 78, 673–684.
Nocita, M., Stevens, A., van Wesemael, B., Aitkenhead, M., Bachmann jj, M., Barth es, B., Ben Dor, E., Brown xx, D., Clairotte, M., Csorba, A., Dardenne jjjj, P., Demattê, J., Genot, V., Guerrero, C., Knadel xxx, M., Montanarella, L., Noon, C., Ramirez-Lopez, L., Robertson, J., Sakai jjjjjj, H., Soriano-Disla, J., Shepherd, K., Stenberg xxxx, B., Towett, E., Vargas, R., Wetterlind xxxx, J., Paulo, S., 2015. Soil spectroscopy: an alternative to wet chemistry for soil monitoring. Adv. Agron. 132, 139–159. https://doi.org/10.1016/bs.agron.2015.02.002.
O'Rourke, S.M., Holden, N.M., 2011. Optical sensing and chemometric analysis of soil organic carbon–a cost effective alternative to conventional laboratory methods? Soil Use Manag. 27, 143–155.
Ouyang, Y., Higman, J., Campbell, D., Davis, J., 2003. Three-dimensional kriging analysis of sediment mercury distribution: a case study. J. Am. Water Resour. Assoc. 39, 689–702. https://doi.org/10.1111/j.1752-1688.2003.tb03685.x.
Pebesma, E., Heuvelink, G., 2016. Spatio-temporal interpolation using Gstat. RFID J 8, 204–218.
R Core Team, 2018. R: A Language and Environment for Statistical Computing.
Robinson, T.P., Metternicht, G., 2006. Testing the performance of spatial interpolation techniques for mapping soil properties. Comput. Electron. Agric. 50, 97–108. https://doi.org/10.1016/j.compag.2005.07.003.
Roudier, P., 2014. Clhs-package Conditioned Latin Hypercube Sampling.
Santra, P., Kumar, M., Panwar, N., 2017. Digital soil mapping of sand content in arid western India through geostatistical approaches. Geoderma Reg 9, 56–72.
Shen, W., Li, M., Huang, C., Wei, A., 2016. Quantifying live aboveground biomass and Forest disturbance of mountainous natural and plantation forests in Northern Guangdong, China, based on multi-temporal Landsat, PALSAR and field plot data. Wenjuan. Remote Sens. 8, 1–24. https://doi.org/10.3390/rs8070595.
Simbahan, G.C., Dobermann, A., 2006. Sampling optimization based on secondary information and its utilization in soil carbon mapping. Geoderma 133, 345–362.
Suk Lee, W., Ehsani, R., 2015. Sensing systems for precision agriculture in Florida. Comput. Electron. Agric. 112 (2–9). https://doi.org/10.1016/j.compag.2014.11.005.
Vågen, T.-G., Winowiecki, L.A., Tondoh, J.E., Desta, L.T., Gumbricht, T., 2016. Mapping of soil properties and land degradation risk in Africa using MODIS reflectance. Geoderma 263, 216–225. https://doi.org/10.1016/j.geoderma.2015.06.023.
Viscarra Rossel, R.A., Walvoort, D.J.J., Mcbratney, A.B., Janik, L.J., Skjemstad, J.O., 2006. Visible, near infrared, mid infrared or combined diffuse reflectance spectroscopy for simultaneous assessment of various soil properties. Geoderma 131, 59–75. https://doi.org/10.1016/j.geoderma.2005.03.007.
Wackernagel, H., 2003. Multivariate Geostatistics: An Introduction with Applications, 3rd ed. Springer-Verlag, Berlin Heidelberg.
Winowiecki, L., Vågen, T.-G., Huising, J., 2016. Effects of land cover on ecosystem services in Tanzania: a spatial assessment of soil organic carbon. Geoderma 263, 274–283. https://doi.org/10.1016/j.geoderma.2015.03.010.
Zhu, Q., Lin, H.S., 2010. Comparing ordinary kriging and regression kriging for soil properties in contrasting landscapes. Pedosphere 20, 594–606. https://doi.org/10.1016/S1002-0160(10)60049-5.